CHAPTER 6

Morphology of 15mer Duplexes Tethered to Au(111) Probed Using Scanning Probe Microscopy

Adapted from Boon, E.M., Barton, J.K., Sam, M., Hill, M.G., Spain, E.M. (2001) *Langmuir*, 17, 5727.

M.S. recorded most of the AFM images.

INTRODUCTION

To fully realize the use of immobilized deoxyribose nucleic acid (DNA) films in biosensing or nanotechnology (1-6), fundamental measurements of their physical properties must be made and interpreted. Formation of DNA films relies on the spontaneous chemisorption of short, thiol-modified oligonucleotides (3-5) or duplexes (6) under buffer solution. Quantitative surface coverage measurements have been obtained for immobilized oligonucleotides with neutron reflectivity, radioisotopic labeling, and electrochemistry (3,7,8). Some fine tuning of the structure of the resulting films has also been achieved (8). In addition, the kinetics of hybridization at the surface of chemically-modified oligonucleotides have been studied with surface plasmon resonance spectroscopy (1,4). From these studies, it was found that desorption and diffusion as well as adsorption must be considered in the kinetics of self-assembly (4). Furthermore, hybridization efficiency was correlated to surface coverage and structure (5). Less is known about the self-assembly mechanism and film structure of thiol-modified DNA duplexes.

We have studied films formed from 5′ linked 15 base pair duplexes and found them to orient their helical axes at approximately 45^{o} with respect to the surface normal (6). No long range morphology was observed via atomic force microscopy (AFM), however. Here we extend these microscopy investigations to study the effect of linkage placement on duplex film formation. We present evidence that the nature of the linker can dramatically affect the morphology of the resulting film. Additionally, we demonstrate the

effectiveness of using a chemically modified tip in investigating film structure by scanning probe microscopy (SPM) and suggest how these chemically-modified duplexes self-assemble on gold surfaces.

MATERIALS AND METHODS

Materials

Unless otherwise indicated, all reagents and solvents were purchased in their highest available purity and used without further purification. All DNA synthesis reagents were obtained from Glen Research. Millipore milliQ (18 M cm) water was used in all experiments. All plasticware was purchased DNase, RNase, and metal free (Sorenson Bioscience, Inc.). All AFM materials were purchased from Digital Instruments, Santa Barbara, CA. Gold wire was obtained from Alfa Aesar.

Preparation of DNA-modified surfaces

Thiol-modified oligonucleotides were prepared as described in the Appendix. Figure 6.1 displays two similar linkages, attached at the 3′ and 5′ carbons of the 15mer duplex, respectively. After stringent purification, the thiol-modified single strand was hybridized with its unmodified complement by combining equimolar amounts of each strand (in 5 mM phosphate, 50 mM NaCl buffer, pH 7) for a final solution of 0.1 mM duplex. This solution was degassed and blanketed with Ar, heated to 90°C for 5 minutes and then

Figure 6.1. Chemical structures of the linkers compared in these studies. A 15mer duplex is tethered to a Au(111) surface via a 3′ (left) and 5′ (right) attachment.

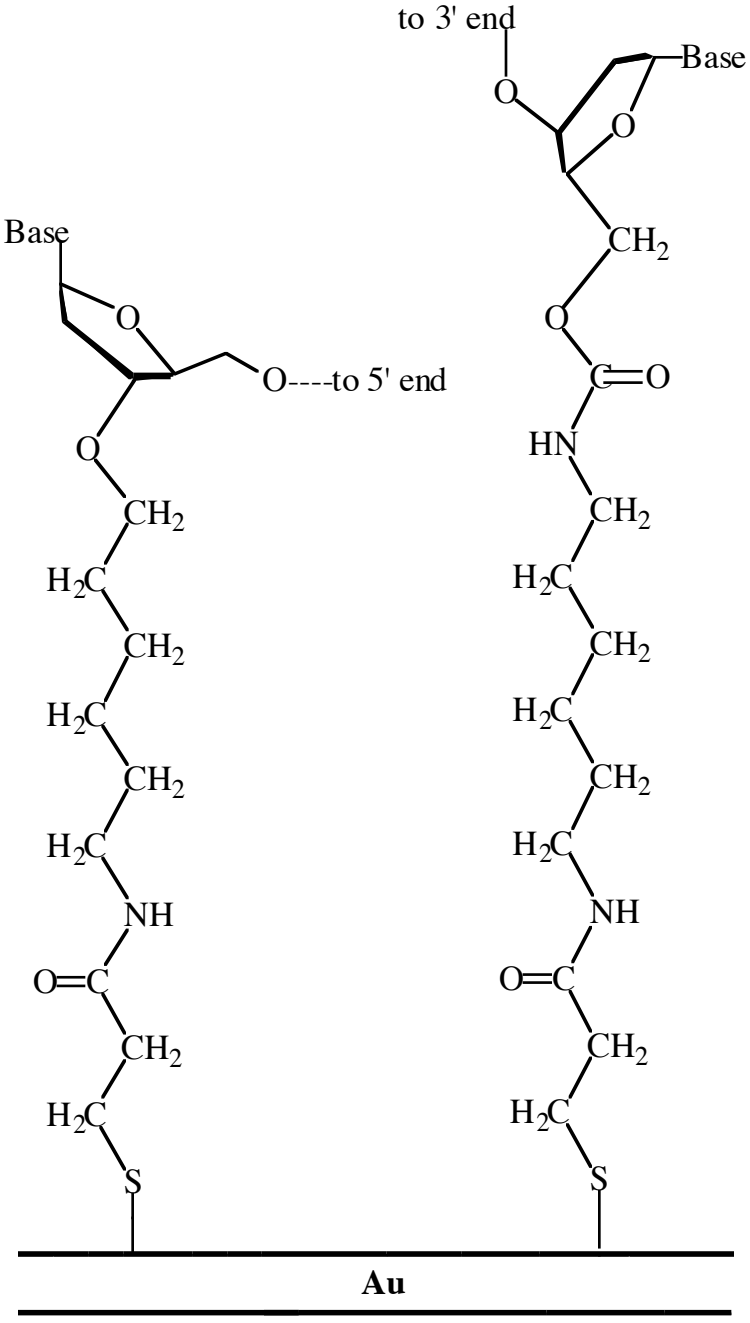

cooled slowly to room temperature (2-3 hours). Just before deposition on the gold surfaces, 0.1 M $MgCl_2$ was added to each sample.

Preparation of AFM samples

Facets on gold balls were prepared by melting a piece of high purity, gold wire in an oxygen-hydrogen flame and then annealing them in an ultrapure hydrogen flame. It has been reported that surfaces formed in this manner are Au (111) facets (12). In the past, we have measured the (111) plane of hydrogen-annealed, vapor deposited Au films on mica with AFM (data not shown). The gold ball was anchored to a stainless steel mounting disk with a facet on top, by piercing the tail of the ball through a septum that was adhered to the disk. Next, 5 μL of 0.1mM thiol-derivatized DNA (5 mM phosphate buffer at pH 7, 0.1M $MgCl_2$) was deposited on top of the ball and incubated for at least 24 hours.

Samples were thoroughly rinsed with phosphate buffer and mounted on a MultiMode Scanning Probe Microscope with Nanoscope IIIa controller (Digital Instruments, Santa Barbara, CA). Commercially available oxide-sharpened Si_3N_4 probes (radius of curvature approximately 5 to 40 nm; Digital Instruments, Santa Barbara, CA) were used with a nominal force constant (0.12 or 0.06 N/m). For imaging with a chemically-modified tip, tips were modified using the following procedure. Tips were coated with 20 Å of Cr and 100 Å of Au, respectively, from an evaporative source under ultrahigh vacuum. The coated tips were then immersed in a 10 mM solution of dodecanethiol for 30 minutes and washed thoroughly with HPLC grade methanol and water.

AFM measurements

Scanning probe microscopy (SPM) images were obtained with bare and chemically modified tips, respectively. All images were collected in contact mode under phosphate buffer (pH 7) at room temperature. Because these films are formed and electrochemically studied in buffer, their properties must be probed in water. These films are quite different from other investigations where unmodified oligomer solutions are evaporated or applied to a surface and imaged in air or vacuum (13). Attempts were made to image with intermittent contact (or tapping) mode under buffer. We never achieved the resolution observed with contact mode, however. When sharp, bare or modified tips were employed in these intermittent contact studies (Olympus tips, radius of curvature less than 20 nm; Digital Instruments, Santa Barbara, CA), the image quality was low and the tip quickly extended into the film (data is not shown). In contact mode, the cantilever deflection feedback set point was continually adjusted during imaging to ensure that a minimum force was applied. Images were collected in height mode (constant cantilever force). Figures 6.2 through 6.4 were subjected to just one modification; the vertical offset between scan lines was removed. For a given image, this was accomplished by subtraction of the average vertical value of the scan line from each point in the scan line. Instrument software provided this modification procedure. No other modifications to the images were performed.

Molecular modeling

Molecular mechanics computations were performed by MacSpartan Pro/Plus (version 2.0) from Wavefunction, Incorporated. For each energy minimization computation, a 12mer duplex crystal structure was imported and its nuclei frozen. The two linkers were attached within the software and the energy was minimized with a MMFF basis set. The crystal structure for the 12mer duplex was obtained from http://www.ncbi.nlm.nih.gov. The file name is 1dnm.pdb; the waters were removed.

RESULTS AND DISCUSSION

DNA-modified Au(111) surfaces were made with both 3′ and 5′ linkers and their surface structure was studied by SPM with bare silicon nitride and chemically modified probes. In Figure 6.2 (a), an SPM image collected with a bare tip is shown for the 5′ linked duplex at a 500 nm x 500 nm magnification. A smooth, essentially featureless film is observed. The terraces observed in Figures 6.2 (a) and (b) are representative of the underlying Au surface. The companion SPM image collected from the same sample with a chemically modified tip is displayed in Figure 6.2 (b). Again, a relatively featureless film composed of the 5′ linked duplexes is measured. These results are in agreement with our previous contact AFM images in buffer of 5′ linked films (6).

The same experiment was repeated with surfaces formed from the 3′ linked duplexes. The respective SPM images are displayed in Figures 6.3 (a) and (b) at a 1 μm x 1 μm magnification. In Figure 6.3 (a), the SPM image obtained with a bare tip shows a slight indication of a film pattern. However, the corresponding SPM image obtained with the chemically modified tip in Figure 6.3 (b) clearly displays a self-assembled pattern. These features are irregular circles (perhaps hexagons) and most have inner diameter dimensions of 8 to 10 nm. The dark part of the image corresponds to the bare gold surface. The light part of the image (the circle perimeters) corresponds to the duplex film, where the increased deflection of the cantilever records a height change in the topographic image. At the higher magnification of 300 nm x 300 nm shown in Figure 6.4, the difference between the bare tip SPM image of Figure 6.4 (a) and the chemically-modified tip image of Figure 6.4 (b) is definite. In some areas of the film, the circles (hexagons) appear close packed.

Following SPM morphology measurements, we measured film height from the Au surface using a method described previously (6). This method of measuring film height was found to be consistent with that measured from ellipsometry (9), and SPM is considered a robust technique for accurate height measurement of features on a surface (13,14). Briefly, under increased force, a bare tip is used to plow a hole into the film. The tip is retracted and re-engaged at the minimum force necessary to obtain an image. The film height is measured between the top of the film and the bottom of the hole, presumed to be the underlying Au surface. The 5′ linked duplexes form a film of height 4.2 ± 0.2 nm, in agreement with our previous measurement of

Figure 6.2. SPM images collected with (a) bare and (b) chemically modified tips of the 5′ duplex in buffer solution (500 nm x 500 nm, height contrast 5 nm). Scale bar in (a) applies to (b).

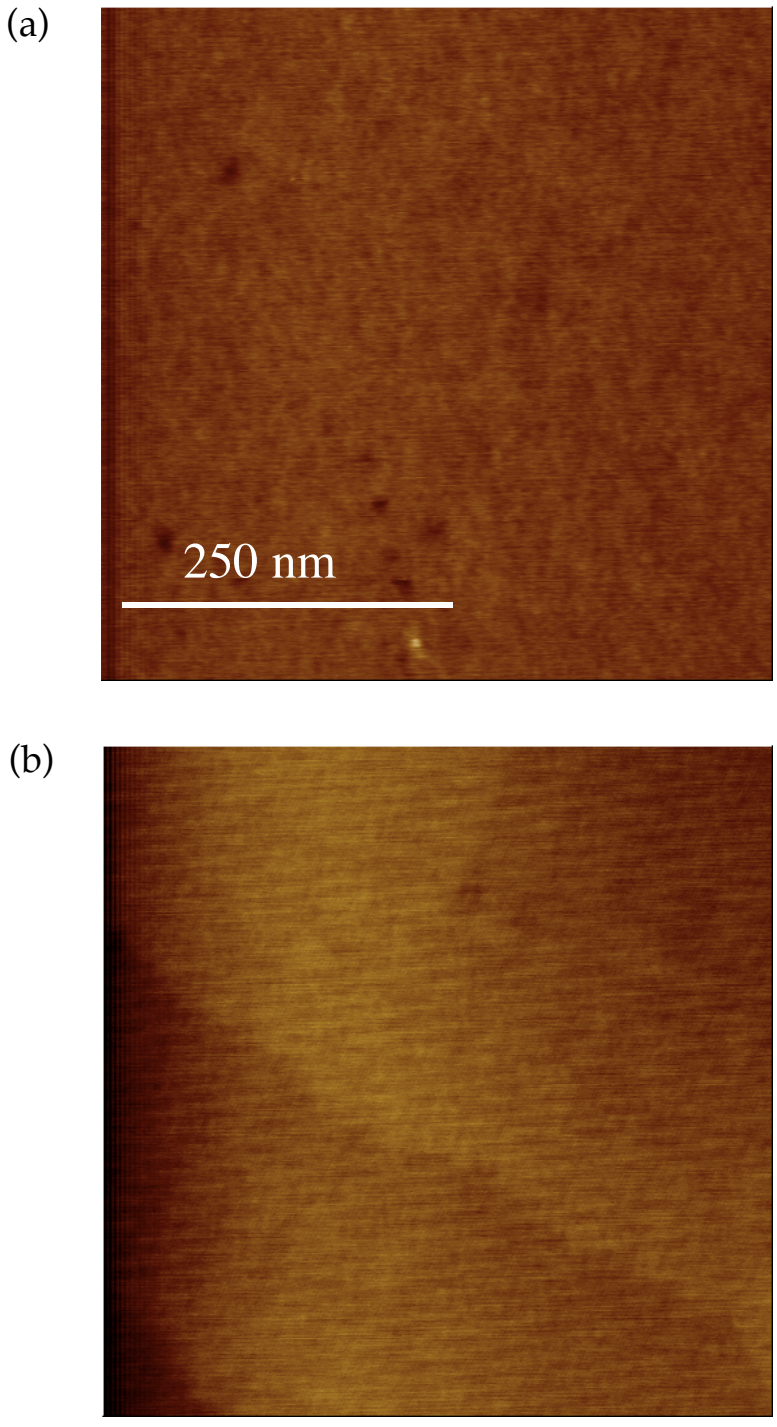

Figure 6.3. SPM images collected with (a) bare and (b) chemically modified tips of the 3′ duplex in buffer solution (1 μm x 1 μm, height contrast 5 nm). Scale bar in (a) applies to (b).

(a)

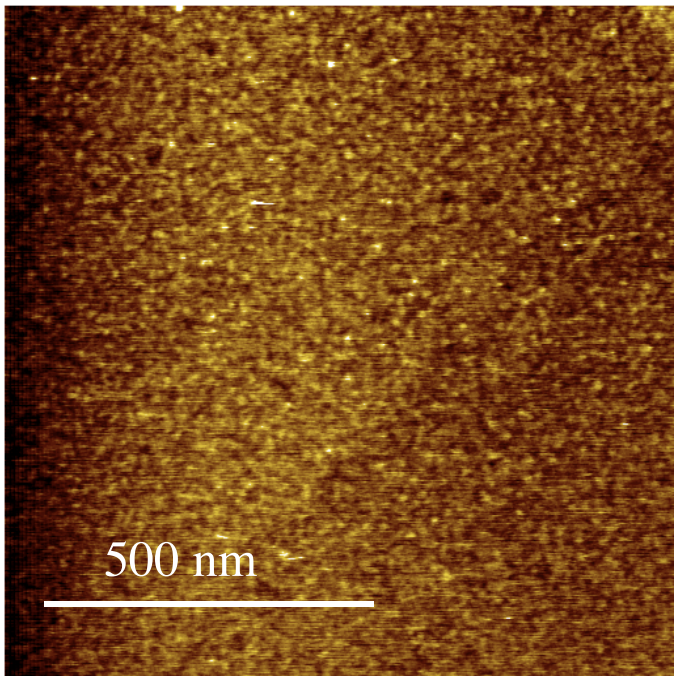

(b)

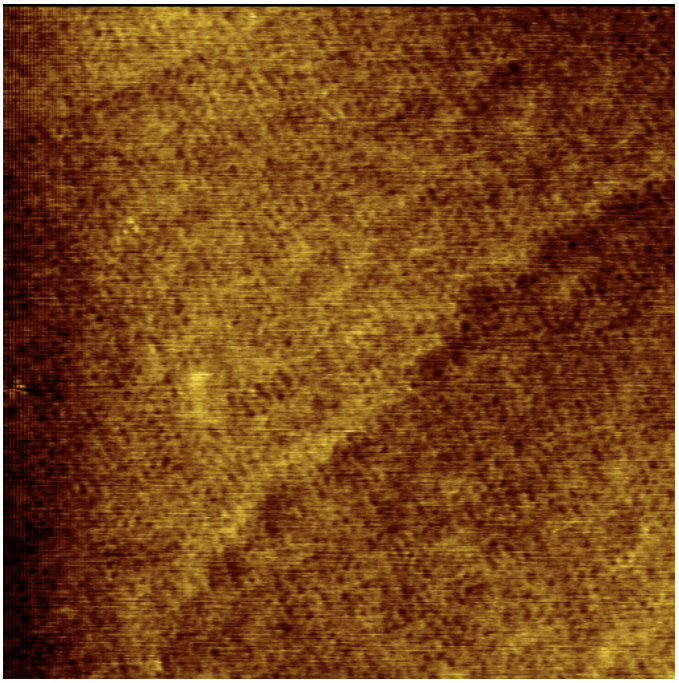

Figure 6.4. SPM images collected with (a) bare (height contrast 5 nm) and (b) chemically modified (height contrast 2.5 nm) tips of the 3′ duplex in buffer solution (300 nm x 300 nm). Scale bar in (a) applies to (b).

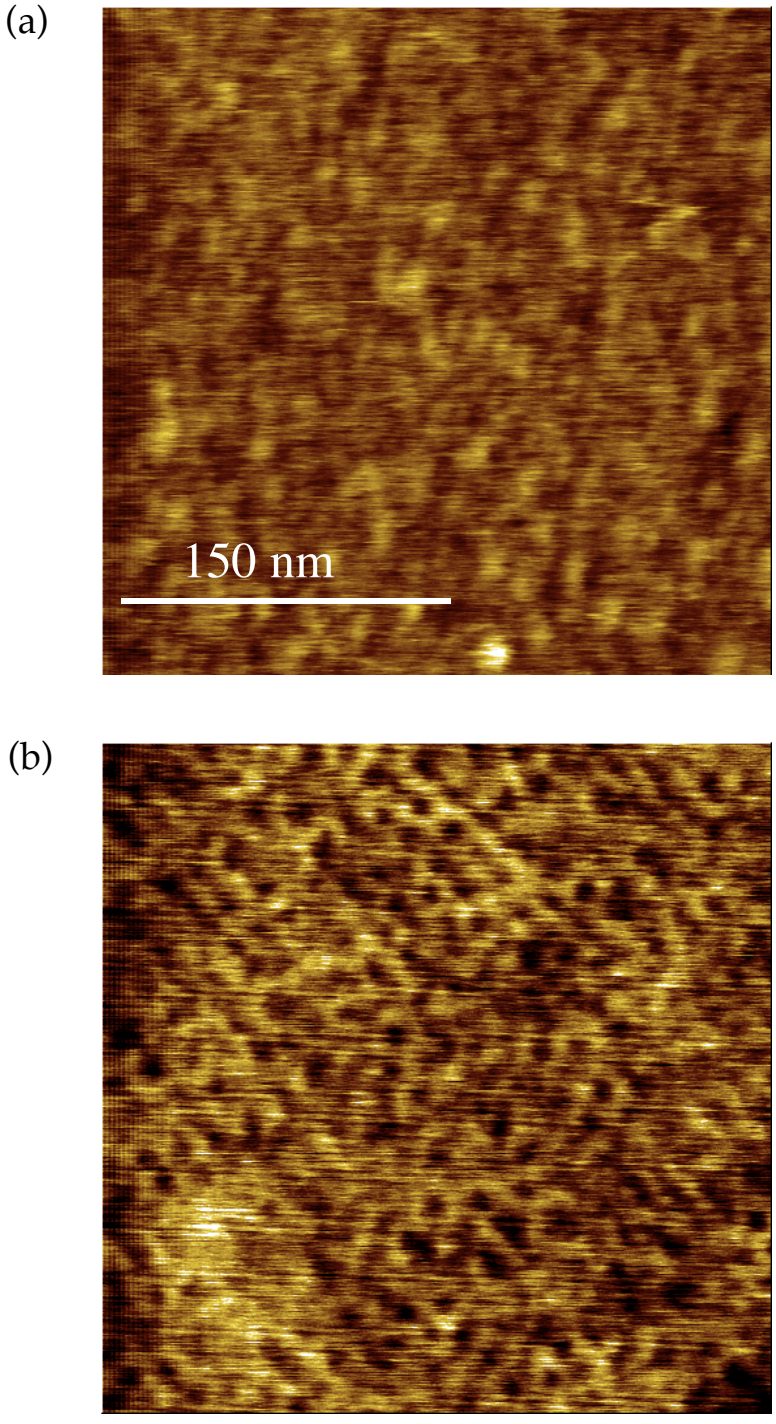

4.5 ± 0.3 nm for 15mer duplexes oriented at an angle of approximately 45° (6). However, the film formed from the 3′ linked duplexes measures 2.0 ± 0.2 nm, a dimension consistent with the diameter of a duplex. Therefore, we conclude that unlike the 5′ linked duplexes, the 3′ linked duplexes lie flat on the surface.

The chemically-modified tip allows resolution of the 3′ linked duplex film. We surmise that this resolution success may be attributed to two factors. First, it is possible that the larger radius of curvature or bluntness of the tip due to alkanethiol adsorption may effectively spread the total force between tip and film contact over a correspondingly larger area. Second, the chemically-modified silicon nitride tip is hydrophobic and neutral. Thus, adhesive forces (15) and the possibility of perturbations due to the diffuse double layer (16) are minimized.

To gain some insight into these film morphology differences, molecular mechanics computations were applied to modified 12mer duplexes. In Figures 6.5 and 6.6, energy minimized molecular models are shown for the 5′ and 3′ linked duplexes, respectively. In each figure, the two structures represent the two lowest energy structures determined from user input initial geometries. These computations do not include effects from water, counterions, or the gold surface. These computed structures are presented only to suggest that linker placement may induce different chain-duplex interactions and possibly affect duplex self-assembly; no definite conclusions can be drawn from them. Figure 6.5 (a) shows the 5′ linker orientation extended from the helical axis of the duplex, while Figure 6.5 (b)

shows it coiled near the end of the duplex. In Figures 6.6 (a) and (b), energy minimized duplexes are shown with the 3′ linkers tucked along the groove in two similar geometries.

With either linker, the first duplexes to assemble likely lie parallel to the surface. As the surface starts to crowd and provided there is enough flexibility or length in the linker, the duplexes might undergo a two dimensional phase transition, as occurs in *n*-alkanethiol film formation (17), and orient at an angle with respect to the surface. Additional duplexes may chemisorb until the surface is optimally packed. We suppose that a two dimensional phase transition in the 5′ linked duplexes might occur because the tethering chain may extend from the duplex parallel to the helical axis. The particular chain-duplex interactions for the 3′ linked species are not known but may restrict these duplexes parallel to the surface and prevent a phase transition.

The absence of phase transition may be considered to be consistent with the observed film pattern of 3′ linked duplexes. In addition, the relatively short linker length may further confine duplex motion parallel to the surface and suggests that there may be a minimum linker length that would allow the 3′ linked duplexes enough flexibility to overcome any chain-duplex interactions.

In conclusion, small changes in linker orientation can greatly affect DNA film structure and this observation must be considered when comparing DNA microarrays from different laboratories. Linker length and composition likely affect these films as well. All of the parameters that affect DNA film structure have not yet been determined, but it is clear that the

Figure 6.5. Two energy minimized models for a 5′ linked 12mer duplex.

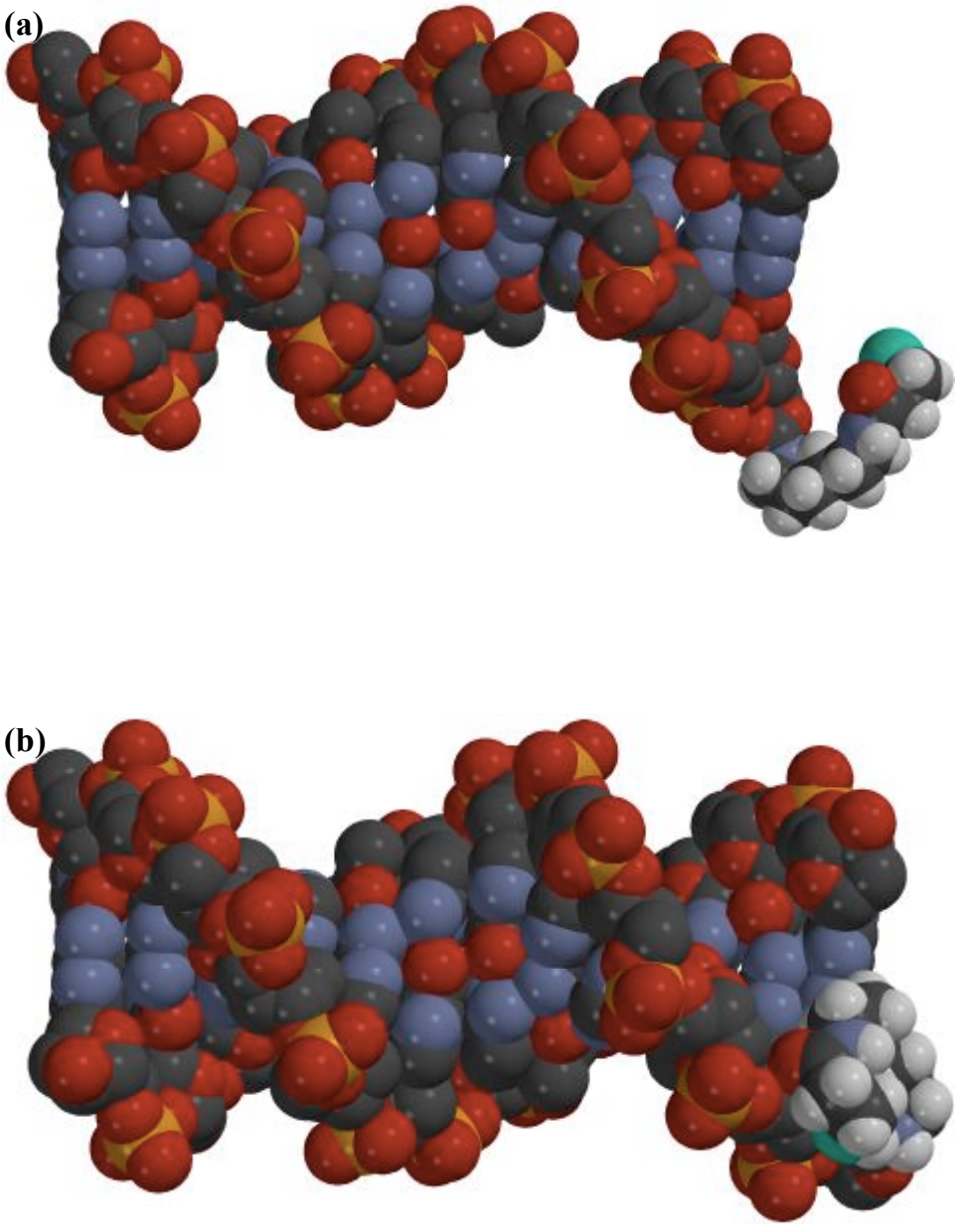

Figure 6.6. Two energy minimized models for a 3′ linked 12mer duplex.

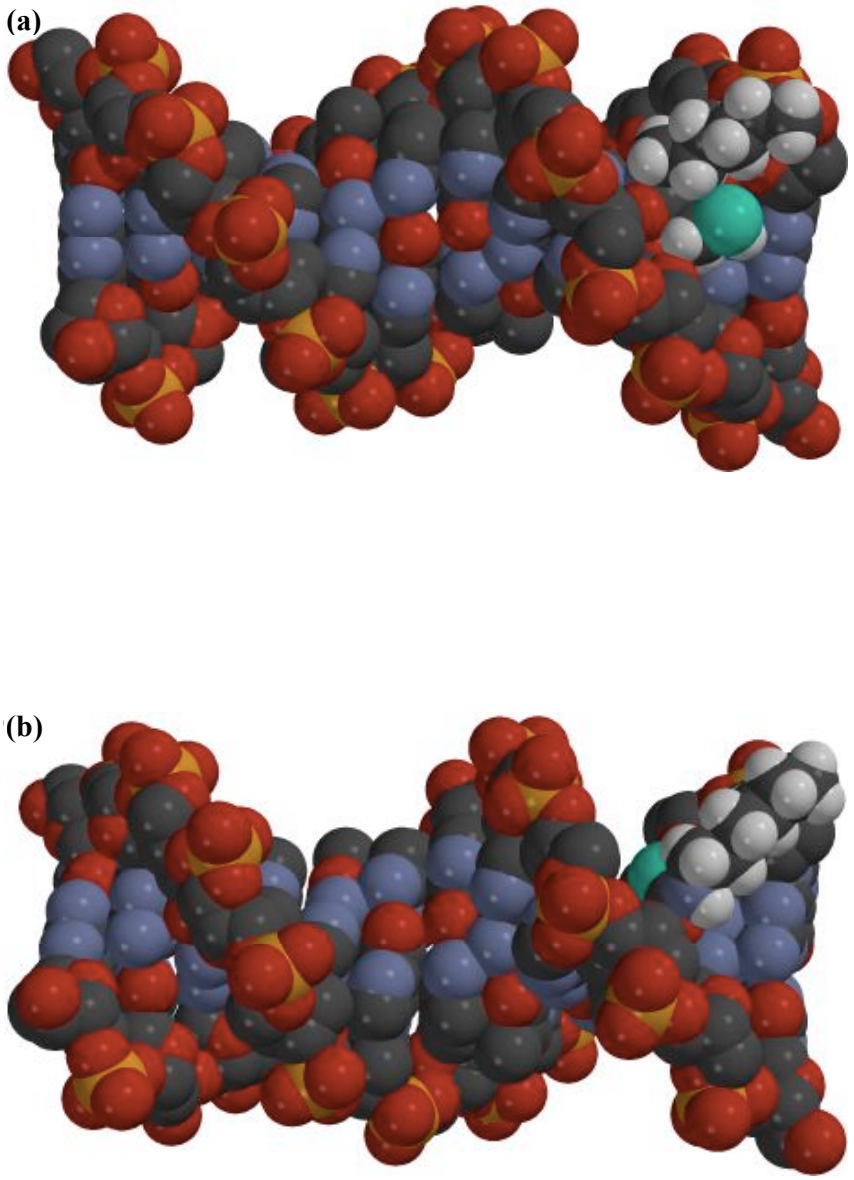

linker between the duplex and the surface can play a major role in determining the organization of the DNA-modified surface.

SUMMARY

The long range film structure of 15 base pair, thiol-derivatized duplexes tethered through single 3′ and 5′ linkages to a Au (111) surface is measured via scanning probe microscopy. Using a hydrophobic, blunt probe routinely yields strong image contrasts that allow long range DNA film structure to be discerned. Film morphology of the 3′ linked duplexes differs from that of its 5′ counterpart as observed by scanning probe microscopy in contact mode under buffer solution. No structural features are distinguished in a film formed with the 5′ linked duplexes as measured with either a bare silicon nitride or chemically-modified probe. However, a distinct pattern in the film structure of the 3′ linked duplexes is measured with a chemically modified, hydrophobic tip; the 3′ linked duplexes lie flat on the surface and form a series of packed circles or hexagons. A hypothesis for the self-assembly mechanism of the 3′ linked duplexes is presented.

REFERENCES

1. Peterlinz, K.A., Georgiadis, R.M., Herne, T.M., Tarlov, M.J. (1997) *J. Am. Chem. Soc. 119*, 3401.

2. Boon, E.M., Ceres, D.M., Drummond, T.G., Hill, M.G., Barton, J.K. (2000) *Nature Biotechnology 18*, 1096.

3. Steel, A.B., Levicky, R.L., Herne, T.M., Tarlov, M.J. (2000) *Biophysical Journal 79*, 975.

4. (a) Peterson, A.W., Heaton, R.J., Georgiadis, R. (2000) *J. Am. Chem. Soc. 122*, 7837. (b) Georgiadis, R., Peterlinz, K.P., Peterson, A.W. (2000) *J. Am. Chem. Soc. 122*, 3166.

5. Huang, E., Satjapipat, M., Han, S., Zhou, F. (2001) *Langmuir 17*, 1215.

6. Kelley, S.O., Barton, J.K., Jackson, N.M., McPherson, L.D., Potter, A.B., Spain, E.M., Allen, M.J., Hill, M.G. (1998) *Langmuir 14*, 6781.

7. Herne, T.M., Tarlov, M.J. (1997) *J. Am. Chem. Soc. 119,* 8916.

8. Levicky, R., Herne, T.M., Tarlov, M.J., Satija, S.K**.** (1998) *J. Am. Chem. Soc. 120*, 9787.

9. Kelley, S.O., Jackson, N.M., Barton, J.K., Hill, M.G. (1997) *Bioconjugate Chem. 8*, 31.

10. Kelley, S.O., Jackson, N.M., Hill, M.G., Barton, J.K. (1999) *Angew. Chem. 38***,** 941.

11. Kelley, S.O., Boon, E.M., Jackson, N.M., Hill, M.G., Barton, J.K. (1999) *Nucleic Acids Res. 27*, 4830.

12. (a) Sawaguchi, T., Yamada, T., Okinaka, Y., Itaya, K. (1995) *J. Phys. Chem. 99*, 14149. (b) Schott, J. Hossick, White, H.S. (1994) *Langmuir 10*, 486.

13. See for example: (a) Hamai, C., Tanaka, H., Kawai, T. (2000) *J. Phys. Chem. B 104*, 9894. (b) Cai, L., Tabata, H., Kawai, T. (2000) *Appl. Phys. Lett. 77*, 3105. (c) Kanno, T., Tanaka, H., Miyoshi, N., Kawai, T. (2000) *Appl. Phys. Lett. 77*, 3848.

14. See for example: Lillehei, P.T., Bottomley, L.A. (2000) *Anal. Chem. 72*, 189.

15. (a) Alley, R.L., Komvopoulos, K., Howe, R.T. (1994) *J. Appl. Phys. 76*, 5731. (b) Tsukruk, V.V., Bliznyuk, V. N. (1998) *Langmuir 14*, 446.

16. (a) Hillier, A.C., Kim, S., Bard, A.J. (1996) *J. Phys. Chem*. *100*, 18808. (b) Hu, K., Bard, A.J. (1997) *Langmuir 13*, 5114. (c) Hu, K., Chai, Z., Whitesell, J.K., Bard, A.J. (1999) *Langmuir 15*, 3343.

17. (a) Poirer, G.E., Pylant, E.D. (1996) *Science 272*, 1145. (b) Xu, S., Liu, G-Y. (1997) *Langmuir 13*, 127. (c) Xu, S., Cruchon-Dupeyrat, S.J.N., Garno J.C., Liu G-Y., Jennings, G.K., Yong, T-H., Laibinis, P.E. (1998) *J. Chem. Phys*. *108*, 5002.